The myristoylation of guanylate cyclase-activating protein-2 causes an increase in thermodynamic stability in the presence but not in the absence of Ca^{2+}

Thomas Schröder, Hauke Lilie, and Christian Lange

Institut für Biochemie und Biotechnologie, Martin-Luther-Universität Halle-Wittenberg, Kurt-Mothes-Str. 3, Halle 06120, Germany

Received 16 January 2011; Revised 8 April 2011; Accepted 11 April 2011
DOI: 10.1002/pro.643
Published online 25 April 2011 proteinscience.org

Abstract: Guanylate cyclase activating protein-2 (GCAP-2) is a Ca^{2+}-binding protein of the neuronal calcium sensor (NCS) family. Ca^{2+}-free GCAP-2 activates the retinal rod outer segment guanylate cyclases ROS-GC1 and 2. Native GCAP-2 is N-terminally myristoylated. Detailed structural information on the Ca^{2+}-dependent conformational switch of GCAP-2 is missing so far, as no atomic resolution structures of the Ca^{2+}-free state have been determined. The role of the myristoyl moiety remains poorly understood. Available functional data is incompatible with a Ca^{2+}-myristoyl switch as observed in the prototype NCS protein, recoverin. For the homologous GCAP-1, a Ca^{2+}-independent sequestration of the myristoyl moiety inside the proteins structure has been proposed. In this article, we compare the thermodynamic stabilities of myristoylated and non-myristoylated GCAP-2 in their Ca^{2+}-bound and Ca^{2+}-free forms, respectively, to gain information on the nature of the Ca^{2+}-dependent conformational switch of the protein and shed some light on the role of its myristoyl group. In the absence of Ca^{2+}, the stability of the myristoylated and non-myristoylated forms was indistinguishable. Ca^{2+} exerted a stabilizing effect on both forms of the protein, which was significantly stronger for myr GCAP-2. The stability data were corroborated by dye binding experiments performed to probe the solvent-accessible hydrophobic surface of the protein. Our results strongly suggest that the myristoyl moiety is permanently solvent-exposed in Ca^{2+}-free GCAP-2, whereas it interacts with a hydrophobic part of the protein's structure in the Ca^{2+}-bound state.

Keywords: protein stability; Ca^{2+}-binding protein; myristoylation; conformational switch; guanylate cyclase-activating protein-2

Introduction

Three isoforms of guanylate cyclase activating proteins, GCAP-1 through -3, have been identified in mammalian photoreceptor cells. All three isoforms of GCAP[1–5] activate both isoforms of retinal guanylate cyclase (ROS-GC1 and 2) at low free Ca^{2+} concentrations. GCAP-2 furthermore inhibits guanylate cyclase activity at the higher levels of Ca^{2+} present in dark-adapted photoreceptor cells.[1,6] ROS-GC 1 and 2 (alternatively GC-E and -F, or retGC-1 and -2) are responsible for the synthesis of cyclic guanosine 3′:5′ monophosphate (cGMP), the second messenger of phototransduction.[7–10] Their GCAP-mediated Ca^{2+}-dependent regulation plays a central role in shaping the photoreceptor light response and in light adaptation (cf., e.g., refs. [11–15]).

GCAP-2, along with its homologs GCAP-1 and -3, belongs to the neuronal calcium sensor (NCS) family within the superfamily of calmodulin-like

Grant sponsor: 3537 A/0903 L (Land Sachsen-Anhalt); GRK1026 (DFG); LA2530/2-1 (DFG).

*Correspondence to: Christian Lange, Institut für Biochemie und Biotechnologie, Martin-Luther-Universität Halle-Wittenberg, Kurt-Mothes-Str. 3, 06120 Halle (Saale), Germany.
E-mail: christian.lange@scilproteins.com

four EF-hand Ca^{2+}-binding proteins. In all NCS proteins, Ca^{2+} binding to EF-hand 1 is disabled by a conserved proline residue in its core loop.[16,17] The other three EF-hands of GCAP-2 are not only able to bind Ca^{2+}, but can also be occupied by Mg^{2+}, when the free Ca^{2+} concentration is low.[18,19]

Like most other members of the NCS proteins, GCAP-2 is myristoylated at the N-terminus.[20] Protein myristoylation is the co-translational covalent attachment of myristic acid[21] or related fatty acids,[22,23] to an N-terminal glycine residue. This eukaryotic lipid modification is performed by a single enzyme, the myristoyl CoA:protein N-myristoyltransferase.[24–26]

The role of myristoylation is best understood for recoverin, the prototype protein of the NCS family. In the Ca^{2+} free state, the myristoyl chain is buried in the hydrophobic interior of the globular protein,[27] whereas upon Ca^{2+} binding, a conformational change of the protein exposes it to the medium.[28,29] The exposure of the fatty acid residue leads to accumulation of the protein at the membrane, where it interacts with its targets. This mechanism, called the Ca^{2+}-myristoyl switch,[30] has been shown to be functional in the NCS proteins neurocalcin δ[31] and hippocalcin[32] as well, but not in NCS-1[33] and KChIP1,[34,35] which show Ca^{2+}-independent membrane association.

In contrast to recoverin, the guanylate cyclase-activating Ca^{2+}-free form of GCAP-2 binds more strongly to membranes than the Ca^{2+}-bound form. The membrane binding of the protein has been reported to be independent of myristoylation.[20,36] On the other hand, surface plasmon resonance measurements showed that the presence of the myristoyl group promoted increased membrane binding of GCAP-2 in the absence of Ca^{2+}.[37] Despite this apparent contradiction, there seems to be agreement that myristoylated GCAP-2 (myr GCAP-2) is a more effective activator of ROS-GC than the non-acylated form (non-myr GCAP-2).[20,37] The detailed tertiary structures of GCAP-2,[38] as well as of its homolog GCAP-3,[39] have only been determined for the non-myristoylated, Ca^{2+}-bound forms. Recently, the structure of Ca^{2+}-bound myristoylated GCAP-1 was solved,[40] showing the myristoyl chain in a hydrophobic pocket. Additionally, fluorescence quenching assays performed with GCAP-1 that had been N-terminally modified with a non-natural, terminally fluorescence-labeled palmitic acid derivative indicated that the lipid moiety was not solvent-accessible in the Ca^{2+}-free state, either. However, the results of a solid-state NMR study showed a high mobility of the myristoyl chain in membrane-bound Ca^{2+}-free GCAP-2.[36]

In summary, all high-resolution structural information available for any of the related guanylate cyclase-activating proteins, GCAP-1 through -3, pertains exclusively to their Ca^{2+} bound states. While functional data clearly indicate a *modus operandi* for the conformational switch of GCAP 2 that is significantly different from recoverin, the structural aspects of the regulation of its target proteins, the retinal guanylate cyclases ROS-GC1 and 2 have remained obscure. No structure of the intracellular part of guanylate cyclase is available, neither alone nor in complex with any GCAP, in any functional state. The binding of GCAP-2 to lipid membranes shows an inverted Ca^{2+} dependence, as compared to recoverin, and is largely independent of the presence of the myristoyl group in GCAP-2. For GCAP-1, it was suggested that the N-terminal fatty acyl group is permanently sequestered inside the protein irrespective of Ca^{2+} load, which would imply a merely structural stabilizing role. On the other hand, myristoylation was found to be a prerequisite for full activation of ROS-GC1 by GCAP-1, indicating a functional interaction between the lipid moiety and the target. In the present work, we set out to investigate the influence of myristoylation on the structural stability of Ca^{2+}-bound and Ca^{2+}-free GCAP-2, to gain information on the nature of the Ca^{2+}-dependent conformational switch of the protein and shed some light on the structural changes associated with Ca^{2+}-binding, especially with respect to the role of the myristoyl group.

Results

Equilibrium folding/unfolding of myr and non-myr GCAP-2

The myristoyl moiety of GCAP-1 was shown to be sequestered in the hydrophobic interior of the protein in its Ca^{2+}-bound state.[40] For the homologous protein GCAP-2, which has ~40% sequence identity to GCAP-1, a similar structural role of the lipid modification may be expected. In such a case, the thermodynamic stability of the non-myristoylated form should be significantly reduced by the lack of the fatty acid side chain, as compared to the stability of myr GCAP-2. No detailed structural information about the Ca^{2+}-free forms of any GCAP is currently available. A comparison of the stability of the myristoylated and non-myristoylated forms under these conditions could potentially provide some insights into the nature of the Ca^{2+}-dependent conformational switch of these proteins. In order to determine the thermodynamic parameters for the folding/unfolding transition of both, myr GCAP-2 and non-myr GCAP-2, in presence and absence of Ca^{2+}, respectively, GuHCl-induced transitions were monitored by CD spectroscopy as well as intrinsic tryptophan fluorescence (Fig. 1). In almost all cases, the obtained curves for unfolding and refolding were superimposable, *i.e.*, all transitions were fully reversible. The only exception was observed for non-myr GCAP-2 in the presence of both, Mg^{2+} and Ca^{2+} (Supporting Information Fig. S1). In this case, refolding resulted in a transition with a midpoint at

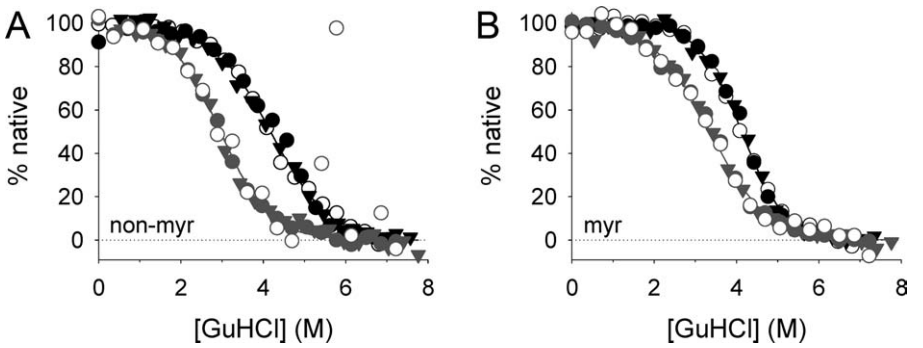

Figure 1. Denaturant-induced folding/unfolding of GCAP-2. Unfolding (circles) and refolding (triangles) transitions of (A) non-myr GCAP-2 and (B) myr GCAP-2 were monitored by far-UV circular dichroism (filled symbols) and tryptophan fluorescence (open symbols), respectively. The depicted experiments were performed without added Mg^{2+} either in the presence of 1 m*M* Ca^{2+} (black) or 1 m*M* EGTA (gray). Solid lines represent curve fits of a two-state unfolding model assuming a linear denaturant dependence of the free energy of unfolding.

a lower GuHCl concentration and less pronounced co-operativity, while in the absence of Mg^{2+} folding/unfolding was fully reversible (Fig. 1) under all conditions. GuHCl-induced folding/unfolding, monitored by CD and unfolding, monitored by intrinsic tryptophan fluorescence at 350 nm showed the same transition midpoints. Furthermore, the same transition midpoints were observed with intrinsic tryptophan fluorescence at different emission wavelengths (not shown). For each condition under which reversible transition curves could be obtained, data was analyzed globally with a two-state unfolding model (Table I). In the presence of 10 m*M* $MgCl_2$ and absence of Ca^{2+}, the stability of myr GCAP-2, as expressed by the standard free energy of unfolding, ΔG^{o}_{U}, was 11.9 kJ/mol. The corresponding value determined for non-myr GCAP-2 was 11.4 kJ/mol. In the presence of Ca^{2+}, the stability of myr GCAP-2 was increased to 18.8 kJ/mol. In the absence of added $MgCl_2$, a stabilization of all forms of GCAP-2 by ~0.3 kJ/mol to 0.9 kJ/mol was observed, and a value for the stability of non-myr GCAP-2 in the absence of Ca^{2+} could be obtained. Remarkably, the Ca^{2+}-dependent stabilization for the non-myristoylated protein was much less pronounced than for myr GCAP-2. While the ΔG^{o}_{U} values for myr (12.2 kJ/mol) and non-myr GCAP-2 (12.3 kJ/mol) were not significantly different in the absence of Ca^{2+}, the value for the Ca^{2+}-bound myristoylated protein (19.6 kJ/mol) was ~4.8 kJ/mol higher than for non-myr GCAP-2 (14.8 kJ/mol). This result might indicate a structurally stabilizing role of the myristoyl moiety in the Ca^{2+}-bound state that is not present in the Ca^{2+}-free protein. This interpretation seems to be supported by a comparison of the co-operativity of unfolding, as expressed by the denaturant *m* value, for the various forms of GCAP-2 (Table I). With a value of 4.8 kJ/mol/M, the highest estimated co-operativity of unfolding was observed for myr GCAP-2 in the presence of Ca^{2+}. The *m* value for Ca^{2+}-bound non-myr GCAP-2, in turn was only 3.6 kJ/mol/M. This was inside the range of the values estimated for the Ca^{2+}-free forms of the protein The greater co-operativity of unfolding for Ca^{2+}-bound myr GCAP-2 indicates the most compact structure and the largest difference in solvent-exposed hydrophobic surface upon folding/unfolding of all forms of the protein.

Putative oligomerization of GCAP-2

In an earlier publication by Olshevskaya et al.,[41] a hypothetical activation mechanism for ROS-GC involving the dimerization of GCAP-2 in the Ca^{2+}-free state was described. Such a mechanism would cause a dependence of the apparent stability, as expressed, e.g., by unfolding transition midpoints, on the protein concentration, and require a different reaction model for the evaluation of the thermodynamic parameters of unfolding. However, the denaturant-induced folding/unfolding curves (cf. above) presented in this work were measured at 14 μg/mL protein concentration for intrinsic tryptophan fluorescence and at 110 μg/mL for far-UV CD, respectively. No change in transition midpoint in response to this nearly eightfold difference in concentration was observed. This indicated that oligomerization had not taken place under the chosen conditions. In order to clarify this point, we decided to perform equilibrium ultracentrifugation experiments with

Table I. *Thermodynamic Parameters of Denaturant-Induced Folding/Unfolding of GCAP-2*

+ Mg^{2+}		ΔG^{o}_{U} (kJ/mol)	*m* (kJ/mol/M)
$-Ca^{2+}$	non-myr	11.4	−3.5
	myr	11.9	−3.5
$+Ca^{2+}$	non-myr	n.d.	n.d.
	myr	18.8	−4.0
$-Mg^{2+}$			
$-Ca^{2+}$	non-myr	12.3	−4.2
	myr	12.2	−3.6
$+Ca^{2+}$	non-myr	14.8	−3.6
	myr	19.6	−4.8

Table II. *Molecular Masses Determined by Analytical Ultracentrifugation of GCAP-2*

$+Mg^{2+}$	M_R (kDa)	[GuHCl] (M)
non-myr	33.8	0
	29.0	1
	22.5	1.25
myr	29.9	0
	24.3	1
$-Mg^{2+}$		
non-myr	28.7	0
	24.0	1
myr	26.5	0
	24.0	1

both, myr GCAP-2 and non-myr GCAP-2, in the absence of Ca^{2+}, a condition, for which dimerization was described and postulated to play a physiological role. The results of these measurements are summarized in Table II. In standard measurement buffer, neither myristoylated nor non-myristoylated GCAP-2 did appear as a homogeneous species. Apparent molecular masses above 25 kDa were observed, indicating the co-existence of monomeric and oligomeric forms of GCAP-2. However, the addition of 1*M* GuHCl led to a complete disaggregation of both forms of GCAP-2. Molecular masses of 23 kDa to 24 kDa were determined, in agreement with monomeric protein. On the basis of these results, an activation mechanism of ROS-GC by dimerization of GCAP-2 cannot be excluded. However, under the conditions of our measurements, oligomerization is not expected to influence the apparent stabilities determined by the performed folding/unfolding equilibrium measurements.

Thermally induced folding/unfolding of myr and non-myr GCAP-2

In order to obtain a more comprehensive characterization of the ligand- and myristoylation-dependent stability of GCAP-2, we performed thermally induced folding/unfolding experiments, monitored by circular dichroism. Initially, we had been unable to observe thermally induced unfolding transitions under any condition, neither spectroscopically nor by means of differential scanning calorimetry (data not shown). We therefore chose to study the thermally induced folding/unfolding of myr GCAP-2 and non-myr GCAP-2 under destabilizing conditions, in the presence of GuHCl (Fig. 2). Because of the observed lack of reversibility for the unfolding of non-myr GCAP-2 in the presence of Mg^{2+} along with Ca^{2+} (cf. above), all represented measurements were performed in buffers without added Mg^{2+}. Under these conditions, the temperature traces observed by far-UV CD were fully reversible in the presence of Ca^{2+}.

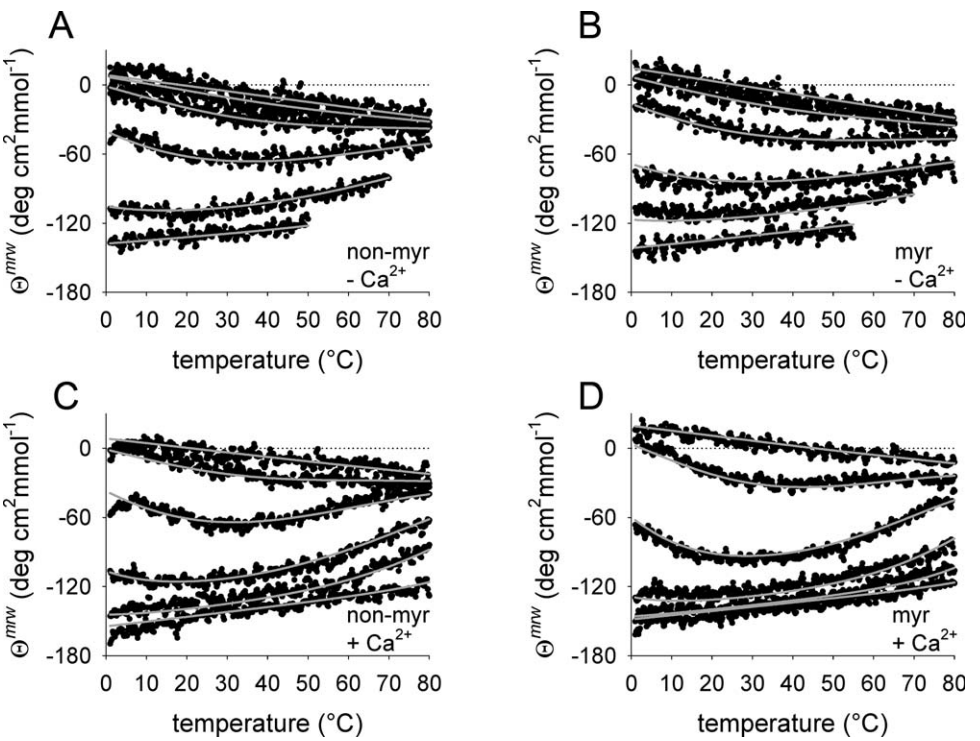

Figure 2. Thermally and denaturant-induced unfolding of GCAP-2. Thermal unfolding transitions of (A) non-myr GCAP-2 and (B) myr GCAP-2 in the presence of 1 m*M* EGTA and 0, 2.0, 3.0, 4.0, 5.0, and 7.1*M* GuHCl (bottom to top) were monitored by far-UV circular dichroism. Analogous experiments were performed for non-myr GCAP-2 (C) and myr GCAP-2 (D) in the presence of 1 m*M* Ca^{2+}. Denaturant concentrations in (C) correspond to (A) and (B), while in the experiment shown in (D), 0.6, 2.0, 3.0, 4.0, 5.0, and 6.9*M* GuHCl (bottom to top) were present. Solid lines represent global curve fits of a two-state unfolding model, as described in the Materials and methods section.

Table III. *Thermodynamic Parameters[a] of Thermally and Denaturant-Induced Unfolding of GCAP-2*

$-Mg^{2+}$		ΔG^{o}_{U} (kJ/mol)	ΔH^{o}_{U} (kJ/mol)	ΔS^{o}_{U} (J/K/mol)	$\Delta C_{p,U}$ (kJ/K/mol)	m (kJ/mol/M)
$-Ca^{2+}$	non-myr	10.7	19.1	28.3	0.72	−3.6
	myr	11.5	10.6	−2.9	0.74	−3.3
$+Ca^{2+}$	non-myr	15.5	26.0	35.1	1.13	−4.0
	myr	20.8	16.1	−15.6	2.23	−4.9

[a] The parameters in the table are given for the reference temperature of 25°C and result from global analyses of two independent sets of experiments for each condition.

In the absence of Ca^{2+}, temperature scans were only reversible up to maximum sample temperatures of 50°C, when no denaturant was present, while protein was lost to aggregation at more elevated temperatures. In the presence of 2*M* GuHCl, however, reversible behavior could be observed up to 70°C, and at GuHCl concentrations of 3*M* or higher, full reversibility was maintained over the entire temperature range of the experiments. The recorded far-UV CD traces showed non-linear temperature dependence with shallow curvatures and inflection points indicative of both hot and cold unfolding of both forms of GCAP-2. Global analysis of the data using a two-state folding/unfolding model (cf. Materials and methods section) allowed for the simultaneous determination of standard free energies, ΔG^{o}_{U}, enthalpies, ΔH^{o}_{U}, and entropies, ΔS^{o}_{U}, of unfolding, along with the change in partial molar heat capacity upon unfolding, $\Delta C_{p,U}$, and the denaturant m value. These values at the chosen reference temperature, 25°C, are reported in Table III. The protein stabilities, as expressed by the ΔG^{o}_{U} values, determined from the thermally induced folding/unfolding experiments, were in good agreement with those obtained by analysis of the denaturant-induced folding/unfolding curves (cf. above). Interestingly, the entropies of unfolding at 25°C were positive, i.e., destabilizing for non-myristoylated GCAP-2, while they were slightly negative for the myristoylated protein, in agreement with a structurally stabilizing role of the hydrophobic myristoyl moiety. As indicated by the shallow slopes and curvatures of the observed temperature traces, and as represented by the calculated theoretical stability curves for myr and non-myr GCAP-2 (Fig. 3), the stability of the various protein forms did not show a very pronounced temperature dependence. The enthalpies of unfolding as well as the changes in heat capacity upon unfolding were found to be significantly smaller than expected for a protein of 204 amino acid residues.[42,43] In the absence of Ca^{2+}, $\Delta C_{p,U}$ for myr and non-myr GCAP-2 was rather similar with 0.76 kJ/K/mol and 0.72 kJ/K/mol, respectively. In the presence of Ca^{2+}, however, the value for the myristoylated protein was 2.24 kJ/

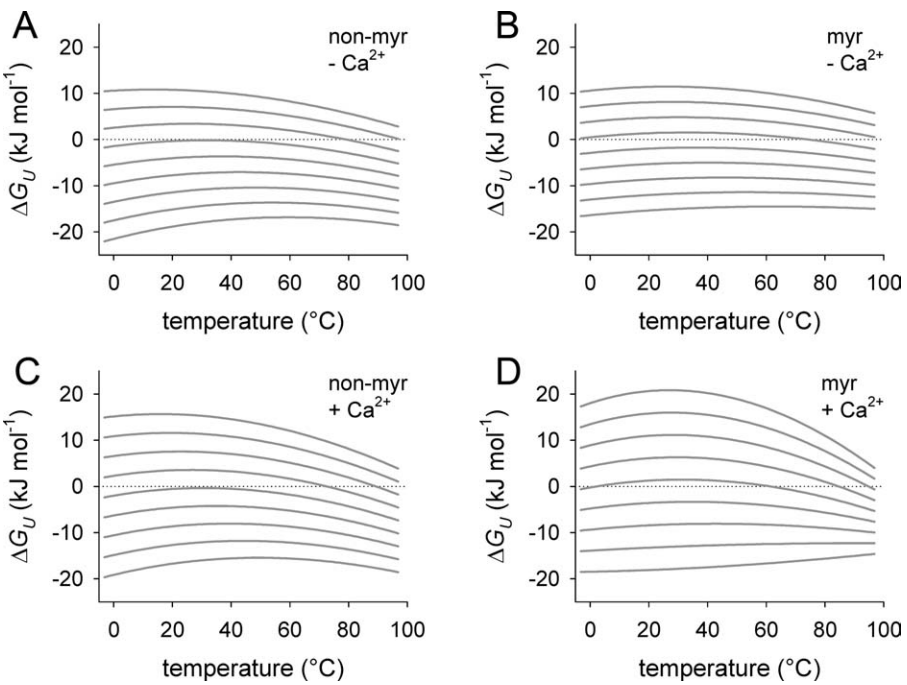

Figure 3. Stability of GCAP-2. The temperature-dependent stability as expressed by the standard free energy of unfolding, ΔG_U, was calculated from the parameters given in Table III for the presence of 0, 1, 2, 3, 4, 5, 6, 7, and 8*M* GuHCl (top to bottom) for non-myr GCAP-2 in the absence of Ca^{2+} (A), myr GCAP-2 in the absence of Ca^{2+} (B), non-myr GCAP-2 in the presence of Ca^{2+} (C), and myr GCAP-2 in the presence of Ca^{2+}(D), respectively.

K/mol, while the value for the non-myristoylated form was only 1.14 kJ/K/mol. For proteins, $\Delta C_{p,U}$ values are generally assumed to be correlated to the change in solvent-accessible hydrophobic surface area upon unfolding, ΔASA. We used the correlation published by Myers et al.[43] to obtain an estimate of the ΔASA values for the various forms of GCAP-2. As expected from the trend in $\Delta C_{p,U}$, the change in exposed hydrophobic area was largest ($\sim$33 nm^2) for Ca^{2+}-bound myristoylated GCAP-2, significantly smaller ($\sim$20 nm^2) for the Ca^{2+}-bound non-myristoylated protein, and smallest ($\sim$16 nm^2) for both forms in the absence of Ca^{2+}. This indicates that the myristoyl chain does not undergo a significant change in solvent exposure upon unfolding of Ca^{2+}-free GCAP-2, in contrast to the Ca^{2+}-bound protein, and therefore is probably fully solvent-exposed in the native state already.

Dye binding experiments

The fluorescent dye 8-anilino-1-naphthalenesulfonic acid (ANS) is known to shift its emission maximum from 515 nm to 479 nm upon binding to hydrophobic patches on protein surfaces.[44] We employed ANS as a spectroscopic probe in order to obtain an additional qualitative estimate of the changes in solvent-exposed hydrophobic surface area between the Ca^{2+}-bound and Ca^{2+}-free states of myr and non-myr GCAP-2 (Fig. 4). When the experiments were performed under the same buffer conditions as the thermally induced folding/unfolding experiments, i.e., without added Mg^{2+}, small but significant differences in ANS fluorescence at 479 nm between Ca^{2+}-bound and Ca^{2+}-free forms were observed. Contrary to expectations, the ANS fluorescence signal was decreased by $\sim$10% in the presence of Ca^{2+}-free non-myr GCAP-2, as compared to the Ca^{2+}-bound protein, while for the myristoylated protein the signal was increased by $\sim$8% in the presence of the Ca^{2+}-free form. This observation for myr GCAP-2 is in agreement with results reported by Gorczyca et al. for the Ca^{2+}-dependent ANS binding of the native bovine protein.[45] When comparing the ANS fluorescence in the presence of myr and non-myr GCAP-2, respectively, it became clear that the influence of the myristoyl group was far greater for the Ca^{2+}-free than for the Ca^{2+}-bound protein [Fig. 4(A)]. In the former case, the non-myristoylated protein only gave rise to less than 80% of the ANS fluorescence observed with myr GCAP-2, while in the latter case, the difference amounted to only about 6% of the total signal. In the presence of added Mg^{2+}, the effects of myristoylation on ANS fluorescence were less pronounced [Fig. 4(B)]. However, Ca^{2+}-free myr and non-myr GCAP-2 still gave rise to significantly different ANS fluorescence signals, while the difference was even further reduced for the Ca^{2+}-bound forms of the protein. In conclusion, the results of the ANS binding experiments suggest that an important

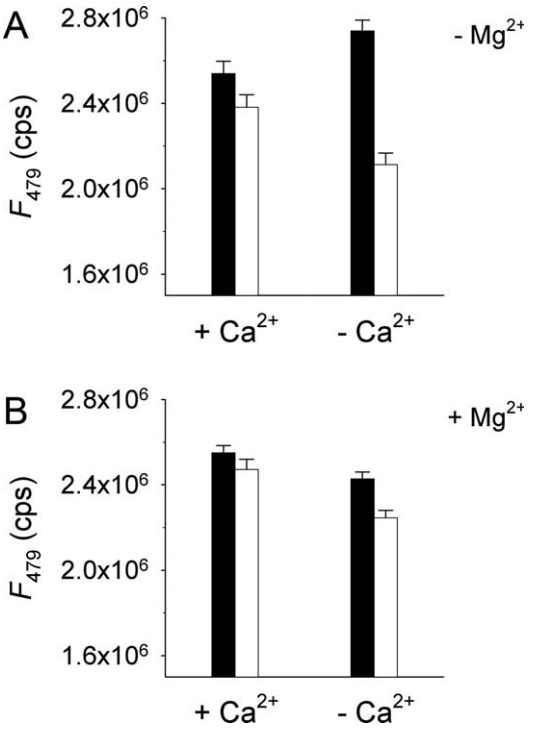

Figure 4. Fluorescent dye binding to GCAP-2. Binding of ANS to myr (black bars) and non-myr (open bars) GCAP-2, respectively, in the presence of 1 m*M* Ca^{2+} ($+Ca^{2+}$) and 1 m*M* EGTA ($-Ca^{2+}$) was monitored by fluorescence spectroscopy in the absence of added Mg^{2+} (A) and in the presence of 10 m*M* Mg^{2+} (B), respectively. Data bars represent mean values $\pm$ standard deviation of six measurements.

difference in solvent-accessible hydrophobic surface area exists between myristoylated and non-myristoylated Ca^{2+}-free GCAP-2, respectively, indicating solvent exposure of the myristoyl moiety in the Ca^{2+}-free conformation, in contrast to the Ca^{2+}-bound form. Under denaturing conditions, in the presence of 6.6*M* GuHCl, ANS binding to the protein was fully suppressed (data not shown).

Discussion

Thermodynamic stability of GCAP-2

We found values for the thermodynamic stability, ΔG^o_U, of GCAP-2 that ranged from 11 kJ/mol for Ca^{2+}-free non-myr GCAP-2 to 21 kJ/mol for the Ca^{2+}-bound myristoylated form. The observed enthalpies of unfolding, ΔH^o_U, were small, while the entropic contribution to unfolding, ΔS^o_U, was almost neutral, indicating a surprisingly low contribution of de-solvation of hydrophobic surface area to the overall stability of the protein. The expected thermodynamic parameters of unfolding for a comparable globular protein of 204 aa at 25°C, according to the correlations assembled in reference 42, would be in the range of $\sim$34 kJ/mol for ΔG^o_U, $\sim$155 kJ/mol for ΔH^o_U, and $\sim$0.41 kJ/K/mol, for ΔS^o_U. As already

mentioned, all these estimates are significantly different from those determined for the various forms of GCAP-2 in this work. The observed heat capacity changes of unfolding, $\Delta C_{p,U}$, (Table III) were also well below the expected value 12 kJ/mol/K for globular proteins of comparable size, and the inferred changes in exposed surface area, ΔASA, even for the Ca^{2+}-bound myristoylated form of GCAP-2, were almost an order of magnitude smaller than the expected value of ~180–200 nm^2.[42,43] In conclusion, the thermodynamic stability data argue strongly against a rigid, compact structure of GCAP-2, and for a highly dynamic protein with a high average exposure of hydrophobic residues even in the native state.

Influence of Mg^{2+}

Intracellular free concentrations of Mg^{2+} are in the order of 0.2 to 3 m*M*,[46] and therefore above the reported K_D values for Mg^{2+} binding, supporting the assumption that the Mg^{2+}-bound forms of GCAP-1 and -2 are the physiological activators of ROS-GC.[18,19] All stability values for GCAP-2 determined in the present work, i.e., the standard free energies of unfolding at 25°C, were decreased by between 0.3 kJ/mol and 0.9 kJ/mol in the presence of 10 m*M* $MgCl_2$. This result was somewhat unexpected, as binding of specific ligands should, in principle, stabilize the native state of a protein. The reported stability of the NCS protein NCS-1, however, was not significantly increased by the presence of Mg^{2+}, either.[47] For both NCSs, this observation might be ascribed to the destabilizing properties of the kosmotropic Mg^{2+} ion or to an ionic strength effect of the added divalent salt. It appears that the net effect of Mg^{2+} on the stability of the relatively acidic proteins is dominated by weak surface interactions, which roughly balance between the folded and unfolded states, respectively, rather than by specific binding to their EF hands. Interestingly, the combined presence of Mg^{2+} and Ca^{2+} in the buffer gave rise to a situation where the denaturant-induced unfolding of non-myristoylated GCAP-2 was not reversible, in contrast to all other tested conditions. The hysteresis observed in this case might be linked to competition of both ions for binding to the EF hands and different binding selectivities in the folded and unfolded state of the protein. Regrettably, this finding precluded a full comparative stability analysis of all forms of GCAP-2 in the presence of Mg^{2+}.

Ca^{2+}- and myristoylation-dependent changes in exposed surface area

The changes in exposed hydrophobic surface area upon unfolding of GCAP-2, as calculated from $\Delta C_{p,U}$, were largest for Ca^{2+}-bound myristoylated GCAP-2, significantly smaller for the Ca^{2+}-bound non-myristoylated protein, and smallest for both forms in the absence of Ca^{2+}. The fact that no difference was observed in this case indicates that the myristoyl chain does not undergo any change in solvent exposure upon unfolding in the in the Ca^{2+}-free state. In the Ca^{2+}-bound state, however, a significantly greater portion of hydrophobic surface is hidden inside the folded structure of the myristoylated protein than in its non-myristoylated form, which might be intuitively ascribed to the myristoyl moiety being sequestered in a hydrophobic binding pocket, in agreement with the available crystal structure of the homologous GCAP-1.[40] These findings were corroborated by the results of the dye binding experiments. While the differences for the Ca^{2+}-bound forms of the protein were small, myristoylated Ca^{2+}-free GCAP-2 showed a significantly higher ANS binding than the non-myristoylated form, in agreement with a solvent-accessible lipid moiety. Taken together, these results would argue for a permanent solvent exposure of the myristoylated N-terminus in Ca^{2+}-free GCAP-2, in striking contrast to the suggested permanent sequestration of the myristoyl moiety in GCAP-1.[40]

Structural role of the myristoyl chain in Ca^{2+}-bound and Ca^{2+}-free GCAP-2

As expected from elementary thermodynamic considerations, and as confirmed for a number of other members of the calmodulin protein superfamily,[47–49] the presence of the ligand Ca^{2+} caused an increase in the observed stability of GCAP-2. However, with 9 kJ/mol *vs*. 5 kJ/mol, this stabilization was almost twice as large for the myristoylated as for the non-myristoylated protein. The difference constitutes one aspect of the central finding of our work, namely that myristoylation increased the thermodynamic stability of GCAP-2 as well as the co-operativity of its folding/unfolding in its Ca^{2+}-bound state, but not in the Ca^{2+}-free state. As already mentioned, the myristoyl moiety of Ca^{2+}-bound GCAP-1 is hidden in the hydrophobic interior of the protein.[40] An equivalent situation in Ca^{2+}-bound GCAP-2, where the lipid chain is sequestered inside the protein, would offer an explanation for the stabilization of its myristoylated in comparison with its non-myristoylated form, as unfolding would require the energetically unfavorable solvation of a comparatively larger extent of hydrophobic surface. However, available ^1H NMR myristoyl difference spectra[50] indicate a certain degree of solvent interaction of the lipid chain in Ca^{2+}-bound myr GCAP-2, arguing against full sequestration of the myristoyl moiety and in favor of a—potentially dynamic—interaction with a surface-exposed feature like a hydrophobic cleft or surface patch. In the Ca^{2+}-free state, the situation is different. The lack of stabilization of myristoylated GCAP-2 with respect to its non-myristoylated form implies that the situation of the lipid moiety in the native, Ca^{2+}-free state is as energetically favorable

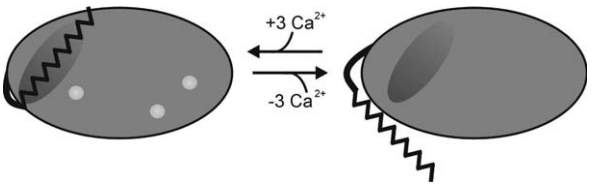

Figure 5. Schematic representation of the Ca^{2+}-dependent conformational switch in GCAP-2. In the Ca^{2+}-bound state (left), the myristoyl moiety interacts with a hydrophobic part of the protein structure and contributes to its structural stability, while in the Ca^{2+}-free state (right), the myristoyl moiety is fully solvent-exposed and makes no net contribution to the free energy of unfolding.

(or unfavorable) as in the corresponding unfolded state. The most straightforward structural explanation for such a behavior is a free, permanently solvent-exposed N-terminus of Ca^{2+}-free GCAP-2. Figure 5 represents a coarse model for a possible Ca^{2+}-dependent conformational shift of the myristoyl moiety in GCAP-2. The idea of a solvent-exposed myristoyl group in Ca^{2+}-free GCAP-2 is in agreement with our previously reported solid state ^2H NMR experiments on the membrane-bound protein,[36] which showed that a major part of the introduced perdeuterated myristoyl chains was inserted in the lipid bilayer, while another part was detectable as isotropic peak, indicating free movement. As implied by this equilibrium between membrane-inserted and freely moving lipid chain, the myristoyl moiety does not significantly contribute to the membrane binding of GCAP-2.[20,36] An exposed lipid moiety, which does not serve the primary purpose of being a membrane anchor, indicates a role of the myristoyl group in the direct interaction with the physiological target proteins of GCAP-2, the retinal guanylate cyclases.

Materials and Methods

Expression and purification of GCAP-2

The protein was expressed in *E. coli* BL21(DE3) from a pET-11a expression vector containing the coding DNA for bovine GCAP-2, (kindly provided by Dr. J.Y. Hwang, Research Center Jülich). Cells were harvested 4 h after induction. Inclusion bodies were isolated and solubilized following established procedures.[51] The following steps were performed at 4°C. Solubilized inclusion body material with a protein concentration of 10 mg/mL in 6*M* guanidinium chloride (GuHCl), pH 3, was refolded by dilution to a final concentration of 150 μg/mL protein in 0.1*M* Tris/HCl, 0.5*M* Na_2SO_4, 1 m*M* $CaCl_2$, 1 m*M* DTT, pH 8.5. After refolding over night, the resulting mixture was cleared by centrifugation and concentrated to ~1 mg/mL using a Vivaflow 200 cross flow ultrafiltration unit (Sartorius AG, Göttingen, Germany), followed by extensive dialysis against 20 m*M* Tris/HCl, pH 8.0. Refolded GCAP-2 was loaded onto a HiTrap Q Sepharose HP anion exchange column (Amersham Biotech, Little Chalfont, UK) and eluted with a linear gradient of 50 m*M* to 1*M* NaCl in 50 m*M* Tris/HCl, 1 m*M* DTT, pH 8.0. The pooled fractions containing the target protein were further purified by size exclusion chromatography on a Superdex 75 XK16/60 column (Amersham Biotech, Little Chalfont, UK) equilibrated with 20 m*M* sodium phosphate buffer, pH 7.0, containing 100 μ*M* $CaCl_2$. In order to obtain myristoylated protein, GCAP-2 was co-expressed with yeast N-myristoyl transferase I, encoded by the plasmid pBB131, as previously described.[52] Myristic acid (50 mg/L) was added to the expression culture at an OD_{600} of 0.4, 30 min before induction. Protein refolding and subsequent ion exchange chromatography were carried out as described above. In order to remove non-myristoylated protein, the pooled fractions containing GCAP-2 were applied to a Nucleosil 500-5 C18 ppn 250/10 reversed phase HPLC column (Macherey & Nagel, Düren, Germany) and eluted by a gradient of 0 to 80% acetonitrile in 0.1% trifluoroacetic acid. The fractions containing myr GCAP-2 were dried in a SpeedVac vacuum concentrator (Thermo Fisher Scientific, Waltham, MA) over night. The dry pellet was dissolved in 6*M* GuHCl, pH 3, and refolded again, as described above. The resulting protein solution was concentrated to ~1.2 mg/mL, followed by extensive dialysis against 100 m*M* cacodylic acid/KOH, 40 m*M* KCl, 10 m*M* $MgCl_2$, 1 m*M* $CaCl_2$, pH 7.0. Homogeneity of all protein samples was monitored by analytical reversed-phase HPLC, and exact molecular masses were determined by ESI-TOF mass spectroscopy. The biological activity of the obtained preparations of myr and non-myr GCAP-2, respectively, was tested by assaying the activation of heterologously expressed ROS-GC1 (cf. Supporting Information Fig. S2).

Heterologous expression of ROS-GC1

HEK293 cells were grown to near confluency in Dulbecco's modified Eagle's medium and transfected with a plasmid containing the cDNA of bovine ROS-GC1 in a pcDNA3.1 vector (kindly provided by Prof. Dr. K.-W. Koch, University of Oldenburg), using lipofectamine transfection reagent (Invitrogen, Carlsbad, CA). Twenty-four hours post transfection, the medium was exchanged and sodium butyrate was added to a final concentration of 7.5 m*M*. Another 24 h later, cells were harvested by a short centrifugation step at (200 g for 5 min), resuspended in PBS and centrifuged again. The cells were resuspended in lysis buffer (10 m*M* Hepes/KOH pH 7.5, 1 m*M* dithiothreitol), disrupted by brief ultrasonication on ice, and the resulting suspension was centrifuged for 5 min at 1000*g* to remove cellular debris. The supernatant was centrifuged at 125,000*g* for 20 min at 4°C to collect the cell membrane fraction. The

membrane pellet was resuspended in buffer containing 10 m*M* Hepes/KOH, pH 7.5, 250 m*M* KCl, 10 m*M* NaCl, and 1 m*M* dithiothreitol. The total protein content of the resulting membrane suspensions was determined by the method of Schaffner and Weissmann.[53]

Guanylate cyclase assay

Guanylate cyclase activity in the obtained HEK293 membrane preparations was determined by a slight modification of an established ROS-GC assay.[54] The assay was performed in a total volume of 50 μL containing 10 μL of the membrane preparations, the indicated amounts of GCAP-2, and EGTA or $CaCl_2$ in final concentrations of 1 m*M*. The reaction was started by addition of 10 μL 5× assay buffer (200 m*M* MOPS/KOH pH 7.1, 280 m*M* KCl; 40 m*M* NaCl; 50 m*M* $MgCl_2$; 10 m*M* GTP) and the mixture was incubated for 30 min at 30°C. The reaction was stopped by addition of an equal volume of 100 m*M* EDTA, pH 7.5, and subsequent incubation at 95°C for 10 min. Precipitated material was removed by centrifugation at 13,000 rpm for 5 min, and the supernatant was applied to a 250 × 4 mm LiChrospher 100 RP18 5 μm reversed-phase HPLC column (Merck KGaA, Darmstadt, Germany). Nucleotides were eluted with a linear gradient of methanol in 5 m*M* KH_2PO_4 at a flow rate of 1.0 mL/min. For detection, the optical extinction at 259 nm was monitored. The peak corresponding to cGMP was integrated and the formed amount was determined from a calibration curve obtained with commercially available cGMP (Sigma-Aldrich, Deisenhofen, Germany).

Denaturant-induced folding/unfolding of GCAP-2

GuHCl-dependent folding and unfolding transitions were measured by far-UV CD spectroscopy. Additionally, unfolding transitions were monitored by observing the fluorescence emission of the aromatic amino acid side chains. All measurements were performed at 25°C in 0.1*M* cacodylic acid/KOH, pH 7.0, 40 m*M* KCl. Measurements with Mg^{2+} additionally contained 10 m*M* $MgCl_2$, measurements with Ca^{2+} additionally contained 1 m*M* $CaCl_2$, measurements without Ca^{2+} additionally contained 1 m*M* EGTA. Before each experiment, the protein at a concentration of ~1.2 mg/mL was extensively dialyzed against the respective buffer. For folding experiments, the dialysis buffers additionally contained 6*M* GuHCl. Out of the resulting stock solutions, the protein was diluted to final concentrations of 0.11 mg/mL for far-UV circular dichroism (CD) spectroscopy, and 14 μg/mL for fluorescence spectroscopy, respectively, into buffers containing the indicated concentrations of GuHCl, which had been prepared from a 8*M* stock solution, confirmed by refractometry.[55] Samples were incubated for 30 min before each measurement. Far-UV CD spectroscopy was performed using a Jasco J-810 spectropolarimeter fitted with a PTC-423S temperature controller (Jasco, Easton, MD) in 1 mm quartz cuvettes. For every sample, the ellipticity at 222 nm was monitored for at least 40 s. The averaged signals over the last 20 s were used for evaluation. Fluorescence measurements were carried out in 1 cm quartz cuvettes using Fluoromax III and IV instruments (Horiba Jobin Yvon, Edison, NJ). Samples were excited at a wavelength of 295 nm, and emission was detected between 310 nm and 400 nm. Spectra were accumulated three times. The signals between 349 nm to 351 nm were averaged and used for evaluation. Data from folding/unfolding transitions monitored by far-UV circular dichroism and unfolding transitions monitored by tryptophan fluorescence were baseline-normalized and analyzed globally for each condition with a two-state unfolding model assuming a linear denaturant dependence of the standard free energy of unfolding, ΔG_U, according to $\Delta G_U = \Delta G^o_U + m$ [GuHCl].

Thermally induced folding/unfolding

For the measurements, protein was dissolved to a final concentration of 0.1 mg/mL in cacodylate buffers (cf. above) containing GuHCl in the indicated concentrations. Thermal scans were performed in 0.5 mm quartz cuvettes with a constant temperature ramp of 1 K/min between 1°C and 80°C in the presence of Ca^{2+}. In the absence of Ca^{2+}, scans were performed between 1°C and 50°C in 0*M* GuHCl, between 1°C and 70°C in 2*M* GuHCl, and between 1°C and 80°C in all other samples. Reversibility of folding/unfolding in these temperature ranges was confirmed by performing repeated up- and downscans. Transitions were monitored by following the far-UV CD signal at a wavelength of 222 nm, as described above. For evaluation, data was normalized to mean molar ellipticity per amino acid residue, Θ^{mrw}.

The temperature traces at all GuHCl concentrations were fitted globally to a two-state folding/unfolding model, assuming temperature-independent molar heat capacity changes of unfolding, $\Delta C_{p,U}$. Baseline drifts for the native and denatured state were treated as linear functions of temperature, and unfolding enthalpy, ΔH^o_U, unfolding entropy, ΔS^o_U, and $\Delta C_{p,U}$ were treated as linear functions of the denaturant concentration.[56]

Analytical ultracentrifugation

For the analytical ultracentrifugation experiments, myr GCAP-2 and non-myr GCAP-2, respectively, were diluted to a final concentration of 0.1 mg/mL in cacodylate buffer without Ca^{2+} and with or without 10 m*M* added $MgCl_2$, containing the indicated concentrations of GuHCl. Experiments were performed at 20°C in a Optima XL-A (Beckman, Palo Alto, CA) centrifuge using double sector cells and an AnTi50

rotor. Sedimentation velocity and equilibrium runs were carried out at a rotor speed of 40,000 rpm and 16,000 rpm, respectively. Optical scans at 280 nm were recorded every 10 min.

Dye binding experiments

Different concentrations of 8-anilino-1-naphthalenesulfonic acid (ANS) were added from a 0.5 m*M* stock solution to samples containing 2.17 μ*M* of myr GCAP-2 and non-myr GCAP-2, respectively, in 0.1*M* cacodylic acid/KOH, pH 7, 1*M* GuHCl, 40 m*M* KCl, and 1 m*M* EGTA. ANS binding to the proteins was monitored by fluorescence spectroscopy. The excitation wavelength was set to 350 nm, and emission spectra were recorded between 400 nm and 550 nm. The signal at 479 nm was used for evaluation. After a first titration experiment, a saturating constant ANS concentration of 0.17 m*M* was used for further studies, in which the binding of the dye to GCAP-2 under different conditions was compared. Buffer composition in these measurements was as described above, with the following exceptions. Samples with Mg^{2+} additionally contained 10 m*M* $MgCl_2$, and samples with Ca^{2+} contained 1 m*M* $CaCl_2$ instead of EGTA. In all cases, two independent experiments were performed, and in each of these experiments, fluorescence intensities were determined in triplicate.

Acknowledgments

The authors extend their thanks to Ms. Amelia Owsicka and Mr. Karol Wyszomyrski for their valuable technical assistance.

References

1. Dizhoor AM, Olshevskaya EV, Henzel WJ, Wong SC, Stults JT, Ankoudinova I, Hurley JB (1995) Cloning, sequencing, and expression of a 24-kDa Ca^{2+}-binding protein activating photoreceptor guanylyl cyclase. J Biol Chem 270:25200–25206.
2. Gorczyca WA, Gray-Keller MP, Detwiler PB, Palczewski K (1994) Purification and physiological evaluation of a guanylate-cyclase activating protein from retinal rods. Proc Natl Acad Sci USA 91:4014–4018.
3. Palczewski K, Subbaraya I, Gorczyca WA, Helekar BS, Ruiz CC, Ohguro H, Huang J, Zhao XY, Crabb JW, Johnson RS, Walsh KA, Gray-Keller MP, Detwiler PB, Baehr W (1994) Molecular cloning and characterization of retinal photoreceptor guanylyl cyclase-activating protein. Neuron 13:395–404.
4. Frins S, Bönigk W, Müller F, Kellner R, Koch KW (1996) Functional characterization of a guanylyl cyclase-activating protein from vertebrate rods—cloning, heterologous expression, and localization. J Biol Chem 271:8022–8027.
5. Haeseleer F, Sokal I, Li N, Pettenati M, Rao N, Bronson D, Wechter R, Baehr W, Palczewski K (1999) Molecular characterization of a third member of the guanylyl cyclase-activating protein subfamily. J Biol Chem 274:6526–6535.
6. Laura RP, Dizhoor AM, Hurley JB (1996) The membrane guanylyl cyclase, retinal guanylyl cyclase-1, is activated through its intracellular domain. J Biol Chem 271:11646–11651.
7. Koch KW (1991) Purification and identification of photoreceptor guanylate cyclase. J Biol Chem 266: 8634–8637.
8. Shyjan AW, Desauvage FJ, Gillett NA, Goeddel DV, Lowe DG (1992) Molecular-cloning of a retina-specific membrane guanylyl cyclase. Neuron 9:727–737.
9. Lowe DG, Dizhoor AM, Liu K, Gu QM, Spencer M, Laura R, Lu L, Hurley JB (1995) Cloning and expression of a second photoreceptor-specific membrane retina guanylyl cyclase (RetGC), RetGC-2. Proc Natl Acad Sci USA 92:5535–5539.
10. Yang RB, Foster DC, Garbers DL, Fülle HJ (1995) Two membrane forms of guanylyl cyclase found in the eye. Proc Natl Acad Sci USA 92:602–606.
11. Koch KW, Stryer L (1988) Highly cooperative feedback control of retinal rod guanylate cyclase by calcium ions. Nature 334:64–66.
12. Pugh EN, Lamb TD (1990) Cyclic GMP and calcium—the internal messengers of excitation and adaptation in vertebrate photoreceptors. Vision Res 30:1923–1948.
13. Gray-Keller MP, Detwiler PB (1994) The calcium feedback signal in the phototransduction cascade of vertebrate rods. Neuron 13:849–861.
14. Fain GL, Matthews HR, Cornwall MC, Koutalos Y (2001) Adaptation in vertebrate photoreceptors. Physiol Rev 81:117–151.
15. Mendez A, Burns ME, Sokal I, Dizhoor AM, Baehr W, Chen J (2001) Role of guanylate cyclase-activating proteins (GCAPs) in setting the flash sensitivity of rod photoreceptors. Proc Natl Acad Sci USA 98:9948–9953.
16. Dizhoor AM, Hurley JB (1999) Regulation of photoreceptor membrane guanylyl cyclases by guanylyl cyclase activator proteins. Methods 19:521–531.
17. Haeseleer F, Imanishi Y, Sokal I, Filipek S, Palczewski K (2002) Calcium-binding proteins: intracellular sensors from the calmodulin superfamily. Biochem Biophys Res Commun 290:615–623.
18. Peshenko IV, Dizhoor AM (2004) Guanylyl cyclase-activating proteins (GCAPs) are Ca^{2+}/Mg^{2+} sensors—implications for photoreceptor guanylyl cyclase (RetGC) regulation in mammalian photoreceptors. J Biol Chem 279:16903–16906.
19. Peshenko IV, Dizhoor AM (2006) Ca^{2+} and Mg^{2+} binding properties of GCAP-1—evidence that Mg2+-bound form is the physiological activator of photoreceptor guanylyl cyclase. J Biol Chem 281:23830–23841.
20. Olshevskaya EV, Hughes RE, Hurley JB, Dizhoor AM (1997) Calcium binding, but not a calcium-myristoyl switch, controls the ability of guanylyl cyclase-activating protein GCAP-2 to regulate photoreceptor guanylyl cyclase. J Biol Chem 272:14327–14333.
21. Wilcox C, Hu JS, Olson EN (1987) Acylation of proteins with myristic acid occurs cotranslationally. Science 238: 1275–1278.
22. Neubert TA, Johnson RS, Hurley JB, Walsh KA (1992) The rod transducin alpha subunit amino terminus is heterogeneously fatty acylated. J Biol Chem 267:18274–18277.
23. Dizhoor AM, Ericsson LH, Johnson RS, Kumar S, Olshevskaya E, Zozulya S, Neubert, TA, Stryer L, Hurley JB, Walsh KA (1992) The NH_2 terminus of retinal recoverin is acylated by a small family of fatty acids. J Biol Chem 267:16033–16036.
24. Towler DA, Adams SP, Eubanks SR, Towery DS, Jackson-Machelski E, Glaser L, Gordon JI (1987) Purification and characterization of yeast myristoyl-CoA-protein N-myristoyltransferase. Proc Natl Acad Sci USA 84:2708–2712.

25. Duronio RJ, Towler DA, Heuckeroth RO, Gordon JI (1989) Disruption of the yeast N-myristoyl transferase gene causes recessive lethality. Science 243:796–800.
26. Glover CJ, Goddard C, Felsted RL (1988) N-Myristoylation of p60Src – identification of a myristoyl-CoA-glycylpeptide N-myristoyltransferase in rat tissues. Biochem J 250:485–491.
27. Tanaka T, Ames JB, Harvey TS, Stryer L, Ikura M (1995) Sequestration of the membrane-targeting myristoyl group of recoverin in the calcium-free state. Nature 376:444–447.
28. Ames JB, Ishima R, Tanaka T, Gordon JI, Stryer L, Ikura M (1997) Molecular mechanics of calcium-myristoyl switches. Nature 389:198–202.
29. Hughes RE, Brzovic PS, Klevit RE, Hurley JB (1995) Calcium-dependent solvation of the myristoyl group of recoverin. Biochemistry 34:11410–11416.
30. Zozulya S, Stryer L (1992) Calcium myristoyl protein switch. Proc Natl Acad Sci USA 89:11569–11573.
31. Ladant D (1995) Calcium and membrane binding properties of bovine neurocalcin delta expressed in Escherichia coli. J Biol Chem 270:3179–3185.
32. Kobayashi M, Takamatsu K, Saitoh S, Noguchi T (1993) Myristoylation of hippocalcin is linked to its calcium-dependent membrane association properties. J Biol Chem 268:18898–18904.
33. McFerran BW, Weiss JL, Burgoyne RD (1999) Neuronal Ca^{2+} sensor 1 – characterization of the myristoylated protein, its cellular effects in permeabilized adrenal chromaffin cells, Ca^{2+}-independent membrane association, and interaction with binding proteins, suggesting a role in rapid Ca^{2+} signal transduction. J Biol Chem 274:30258–30265.
34. O'Callaghan DW, Hasdemir B, Leighton M, Burgoyne RD (2003) Residues within the myristoylation motif determine intracellular targeting of the neuronal Ca^{2+} sensor protein KChIP1 to post-ER transport vesicles and traffic of Kv4 K^+ channels. J Cell Sci 116:4833–4845.
35. Hasdemir B, Fitzgerald DJ, Prior IA, Tepikin AV, Burgoyne RD (2005) Traffic of Kv4 K^+ channels mediated by KChIP1 is via a novel post-ER vesicular pathway. J Cell Biol 171:459–469.
36. Vogel A, Schröder T, Lange C, Huster D (2007) Characterization of the myristoyl lipid modification of membrane-bound GCAP-2 by ^2H solid-state NMR spectroscopy. Biochim Biophys Acta 1768:3171–3181.
37. Hwang JY, Koch KW (2002) Calcium- and myristoyl-dependent properties of guanylate cyclase-activating protein-1 and protein-2. Biochemistry 41:13021–13028.
38. Ames JB, Dizhoor AM, Ikura M, Palczewski K, Stryer L (1999) Three-dimensional structure of guanylyl cyclase activating protein-2, a calcium-sensitive modulator of photoreceptor guanylyl cyclases. J Biol Chem 274:19329–19337.
39. Stephen R, Palczewski K, Sousa MC (2006) The crystal structure of GCAP3 suggests molecular mechanism of GCAP-linked cone dystrophies. J Mol Biol 359:266–275.
40. Stephen R, Bereta G, Golczak M, Palczewski K, Sousa MC (2007) Stabilizing function for myristoyl group revealed by the crystal structure of a neuronal calcium sensor, guanylate cyclase-activating protein 1. Structure 15:1392–1402.
41. Olshevskaya EV, Ermilov AN, Dizhoor AM (1999) Dimerization of guanylyl cyclase-activating protein and a mechanism of photoreceptor guanylyl cyclase activation. J Biol Chem 274:25583–25587.
42. Robertson AD, Murphy KP (1997) Protein structure and the energetics of protein stability. Chem Rev 97: 1251–1267.
43. Myers JK, Pace CN, Scholtz JM (1995) Denaturant m-values and heat capacity changes—relation to changes in accessible surface areas of protein pnfolding. Protein Sci 4:2138–2148.
44. Stryer L (1965) The interaction of a naphthalene dye with apomyoglobin and apohemoglobin. A fluorescent probe of non-polar binding sites. J Mol Biol 13:482–495.
45. Gorczyca WA, Kobiałka M, Kuropatwa M, Kurowska E (2003) Ca^{2+} differently affects hydrophobic properties of guanylyl cyclase-activating proteins (GCAPs) and recoverin. Acta Biochim Pol 50:367–376.
46. Gunther T (2006) Concentration, compartmentation and metabolic function of intracellular free Mg^{2+}. Magn Res 19:225–236.
47. Aravind P, Chandra K, Reddy PP, Jeromin A, Chary KVR, Sharma Y (2008) Regulatory and structural EF-hand motifs of neuronal calcium sensor-1: Mg^{2+} modulates Ca^{2+} binding, Ca^{2+}-induced conformational changes, and equilibrium unfolding transitions. J Mol Biol 376:1100–1115.
48. Muralidhar D, Jobby MK, Krishnan K, Annapurna V, Chary KVR, Jeromin A, Sharma Y (2005) Equilibrium unfolding of neuronal calcium sensor-1 – N-terminal myristoylation influences unfolding and reduces protein stiffening in the presence of calcium. J Biol Chem 280:15569–15578.
49. Masino L, Martin SR, Bayley PM (2000) Ligand binding and thermodynamic stability of a multidomain protein, calmodulin. Protein Sci 9:1519–1529.
50. Hughes RE, Brzovic PS, Dizhoor AM, Klevit RE, Hurley JB (1998) Ca^{2+}-dependent conformational changes in bovine GCAP-2. Protein Sci 7:2675–2680.
51. Rudolph R, Boehm G, Lilie H, Jaenicke R, Protein function—a practical approach. In: Creighton TE, Ed. (1997) Folding proteins. Oxford: IRL Press, pp 57–99.
52. Duronio RJ, Jackson-Machelski E, Heuckeroth RO, Olins PO, Devine CS, Yonemoto W, Slice LW, Taylor SS, Gordon JI (1990) Protein N-myristoylation in Escherichia coli—reconstitution of a eukaryotic protein modification in bacteria. Proc Natl Acad Sci USA 87: 1506–1510.
53. Schaffner W, Weissman C (1973) Rapid, sensitive, and specific method for determination of protein in dilute solution. Anal Biochem 56:502–514.
54. Lambrecht HG, Koch KW (1992) A 26 kd calcium binding protein from bovine rod outer segments as modulator of photoreceptor guanylate cyclase. EMBO J 10: 793–798.
55. Pace CN (1986) Determination and analysis of urea and guanidine hydrochloride denaturation curves. Methods Enzymol 131:266–280.
56. Dallüge R, Oschmann J, Birkenmeier O, Lücke C, Lilie H, Rudolph R, Lange C (2007) A tetrapeptide fragment-based design method results in highly stable artificial proteins. Proteins 68:839–849.